A new millimeter-wave observation of the weakly bound CO–N2 complex

ARTICLE *in* JOURNAL OF MOLECULAR SPECTROSCOPY · DECEMBER 2014

Impact Factor: 1.48 · DOI: 10.1016/j.jms.2014.12.016

4 AUTHORS, INCLUDING:

Leonid A. Surin
University of Cologne
57 PUBLICATIONS **575** CITATIONS
SEE PROFILE

Alexey Potapov
University of Cologne
32 PUBLICATIONS **166** CITATIONS
SEE PROFILE

Stephan Schlemmer
I. Physikalisches Institut, Universität zu Köln
235 PUBLICATIONS **2,888** CITATIONS
SEE PROFILE

Journal of Molecular Spectroscopy 307 (2015) 54–58

Contents lists available at ScienceDirect

Journal of Molecular Spectroscopy

journal homepage: www.elsevier.com/locate/jms

A new millimeter-wave observation of the weakly bound CO–N_2 complex

L.A. Surin [a,b,*], A. Potapov [a], H.S.P. Müller [a], S. Schlemmer [a]

[a] I. Physikalisches Institut, Universität zu Köln, Zülpicher Str. 77, 50937 Cologne, Germany
[b] Institute of Spectroscopy, Russian Academy of Sciences, 142190 Troitsk, Moscow, Russia

ARTICLE INFO

Article history:
Received 1 December 2014
In revised form 9 December 2014
Available online 17 December 2014

Keywords:
Millimeter-wave spectroscopy
van der Waals complex
CO–N_2 complex
Internal rotor
Quadrupole coupling
OROTRON

ABSTRACT

New millimeter-wave transitions of the CO–N_2 van der Waals complex have been observed using the intracavity OROTRON jet spectrometer in the frequency range of 103–159 GHz. For the less abundant form, CO–*para*N_2, a total of 37 rotational transitions were assigned to three $K = 0$–0, 0–1, 2–1 subbands connecting the $(j_{CO}, j_{N2}) = (1,1)$ and $(j_{CO}, j_{N2}) = (0,1)$ internal rotor states. The upper $K = 0$ and $K = 2$ "stacks" of rotational levels were probed for the first time here by millimeter-wave spectroscopy following a recent infrared study by Rezaei et al. (2013). The observation of new subbands fixes with higher precision not only these upper $K = 0$ and $K = 2$ but also lower $K = 1(f)$ levels, not linked with other stacks in earlier rotational studies. For the more abundant form, CO–*ortho*N_2, five new *P*-branch rotational transitions of the $K = 0$–0 "CO bending" subband are reported, thus extending previous measurements. Nuclear quadrupole hyperfine structure due to the presence of two equivalent ^{14}N nuclei was partly resolved and analyzed to give additional information about the angular orientation of the N_2 molecule in the complex.

1. Introduction

Intermolecular interactions between N_2, the main atmospheric constituent, and CO, a significant atmospheric pollutant, is of natural interest because of their direct relevance to the Earth's atmosphere. The CO–N_2 system is a van der Waals complex, and in general, its bound states are sensitive to the interaction potential. Thus high-resolution spectroscopy of CO–N_2 is an important tool for probing of intermolecular forces.

The experimental studies of the CO–N_2 complex are already quite extensive. First spectra were recorded in the 4.7 μm infrared region of the CO stretching vibration by Kawashima and Nishizawa [1] using a pulsed molecular beam and by Xu and McKellar [2] using a continuous slit-jet nozzle expansion, both combined with a diode laser spectrometer. With the help of the prediction from these infrared works [1,2], the microwave observations [3–5] as well as millimeter-wave study [4] have been made. The rotational spectra [3–5] revealed hyperfine structure due to the presence of two ^{14}N nuclei providing additional information on the average orientation of the N_2 moiety in the complex. These first studies were later continued in the infrared [6] and millimeter-wave [7,8] regions extending the previous tentative assignments and providing further details on the CO–N_2 complex. Recently Rezaei et al. reported a broad-band (2135–2165 cm^{-1}) infrared spectrum of CO–N_2 obtained using a tunable quantum cascade laser [9]. They also summarized all previous studies giving a fairly extensive picture of the CO–N_2 energy levels in both the ground and excited CO vibrational states, $v_{CO} = 0$ and 1.

As in the case of many other weakly-bound complexes (for example, CO–H_2 [10,11]), it is useful to label the energy levels of CO–N_2 using the free rotor numbers corresponding to rotational angular momenta of the constituent monomers, j_{CO} and j_{N2}, even though this rotation is somewhat hindered in the complex. Further, due to symmetry and nuclear spin statistics of the two equivalent atoms in N_2 all levels are separated into two distinct groups corresponding to complexes formed from *ortho*- or *para*-N_2. *Ortho*-N_2, with resultant nuclear spin $I = 0$ or 2, has even values of j_{N2}, while *para*N_2, with $I = 1$, has odd values of j_{N2}.

The first observed CO–*ortho*N_2 spectra involved only the rotation less $j_{N2} = 0$ states (the $j_{N2} = 2$ state was detected only in the latter infrared study [9]), therefore they resembled those of CO–rare gas complexes (e.g. Ne–CO or Ar–CO). Rotational levels occurred in 'stacks' with increasing values of total rotational angular momentum, *J*, and well-defined values of *K*, its projection on the intermolecular axis. Now three such stacks are known for CO–*ortho*N_2 in the ground ($v_{CO} = 0$) state: $K = 0$ ($j_{CO}, j_{N2} = 0, 0$) and

* Corresponding author at: I. Physikalisches Institut, Universität zu Köln, Zülpicher Str. 77, 50937 Cologne, Germany.

http://dx.doi.org/10.1016/j.jms.2014.12.016
0022-2852/

$K = 0, 1$ ($j_{CO}, j_{N2} = 1, 0$). In the excited ($v_{CO} = 1$) state, the three analogous stacks with $K = 0$ and 1 are known, together with additional three stacks with $K = 0, 1, 2$ ($j_{CO}, j_{N2} = 2, 0$) and two stacks with $K = 0, 1$ ($j_{CO}, j_{N2} = 1, 2$). The spectra of CO–*para*N_2 are more complicated because of the presence of N_2 angular momentum ($j_{N2} = 1$) even at lowest energy. Stacks with $K = 0, 1$ ($j_{CO}, j_{N2} = 0, 1$) and $K = 0, 1, 2$ ($j_{CO}, j_{N2} = 1, 1$) are known for $v_{CO} = 0$, and analogous stacks together with two additional stacks with $K = 2$ and 3 (j_{CO}, $j_{N2} = 2, 1$) are known for $v_{CO} = 1$. The origins of observed rotational levels stacks of CO–*ortho*N_2 and CO–*para*N_2 are depicted in Fig. 2 and Fig. 3 of Ref. 9 respectively.

All known stacks of the CO–N_2 complex in the ground $v_{CO} = 0$ state have been well characterized now by microwave and millimeter-wave spectroscopy with exception of two recently observed [9] $K = 0$ and 2 stacks ($j_{CO}, j_{N2} = 1, 1$) of the CO–*para*N_2 spin modification. In this paper we present new survey spectroscopic investigations of CO–N_2 with the OROTRON spectrometer in the frequency range of 103–159 GHz. It resulted, first, in the observations of the $K = 0$–0, $K = 0$–1 and $K = 2$–1 subbands of CO–*para*N_2, that confirmed the detection of the $K = 0$ and 2 stacks in the latest infrared study [9]. Second, for CO–*ortho*N_2 we observed new *P*-branch transitions belonging to the $K = 0$–0 subband, thus extending our previous observation of the CO bending mode [7]. The important aspect of the present study in comparison to infrared results [9] is observation and analysis of N-nuclei quadrupole splitting resolved to a varying degree for the most of the detected lines. These data provide additional information about the angular orientation and dynamics of the N_2 subunit within the complex, that can be used for comparison with the results of *ab initio* calculations.

Until recently the theoretical work on the CO–N_2 intermolecular potential comprised only the semiempirical result reported by Franken and Dykstra [12] and an *ab initio* study of selected structures by Fišer et al. [13,14]. In 2011, Karimi-Jafari et al. [15] reported the first complete four dimensional potential energy surface. The study found the global energy minimum to be planar

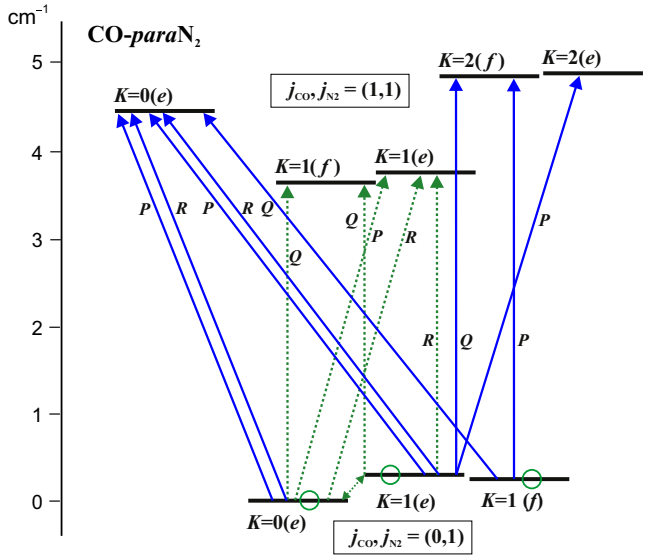

Fig. 1. Rotational energy stacks origins and observed subbands for the CO–*para*N_2 complex for the lowest state (j_{CO}, j_{N2}) = (0,1) and for the upper state (j_{CO}, j_{N2}) = (1,1). The stacks are distinguished by different values of *K*, the projection of the angular momentum *J* on the intermolecular axis. The labels *e* and *f* determine the parity of *J* levels within a given stack. The lowest $J = K = 0$ level is set to zero energy. Previously observed subbands [5,8] are marked by dotted arrows. The states, where pure rotational $\Delta K = 0$ transitions were observed [5], are selected by circles. The new subbands measured in the present work are indicated by solid arrows.

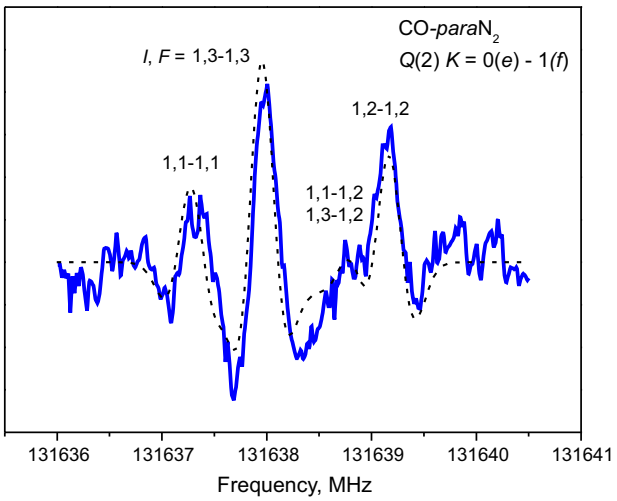

Fig. 2. Recording of the $K = 0(e)$–$1(f)$ $Q(2)$ rotational transition of the CO–*para*N_2 spin modification together with a simulation of the spectrum obtained from the final set of spectroscopic parameters. The nuclear quadrupole structure due to two equivalent ^{14}N nuclei is partly resolved.

with a distorted T-shape in which N_2 forms the 'leg' of the T and the C atom is tilted toward the N_2, and this is the only minimum on the global surface. No bound state calculations have been done so far, that makes difficult a direct comparison between experiment and theory. Such work is in progress now and will be reported separately.

2. Experimental

The millimeter wave spectra of CO–N_2 have been measured in the frequency range of 103–159 GHz using the intracavity jet spectrometer, OROTRON. Details of the set up were given elsewhere [16]. The experiment was performed with a pin-hole pulsed jet source, General Valve, Series 9. The diameter of the nozzle was 1 mm, and the typical repetition rate was 10-15 Hz. We used a gas mixture of 1% of CO and 1% of N_2 in Ne at a backing pressure of 3–4 bar. For most of the absorption measurements, the full linewidth at half maximum (FWHM) was about 300 kHz and the accuracy of line center positions was estimated to be about 50 kHz.

Transitions of the Ne–CO complex and the $(CO)_2$ dimer were also observed in the spectrum but they could be easily distinguished from CO–N_2 lines due to our previous millimeter-wave survey of both, Ne–CO [17] and $(CO)_2$ [18,19]. The hyperfine structure due to two ^{14}N quadrupole nuclei was helpful very often for attributing spectral features to CO–N_2 and for assigning their quantum numbers.

3. Results and analysis

3.1. CO–*para*N_2

As was mentioned above, it is useful to label the energy levels of the CO–N_2 complex in terms of free internal rotors. Each (j_{CO}, j_{N2}) state forms the foundation for a number of stacks of end-over-end rotational levels. The corresponding stack origins are shown for CO–*para*N_2 in Fig. 1. The stacks are distinguished by different values of *K*, projection of total rotational angular momentum *J* on the intermolecular axis. The labels *e* and *f* determine the parity of *J* levels within a given stack. The parity of an even-*J* level is + for stacks labeled by *e* and − for *f*, while the parity of an odd-*J* level is − for *e* and + for stacks labeled by *f*.

Table 1
Assigned $K = 0–0$, $K = 0–1$ and $K = 2–1$ ($j_{CO}, j_{N2} = 1, 1–0, 1$) rotational transitions of CO–*para*N_2, their frequencies[a] and residuals.

$J'–J''$	$I', F'–I'', F''$	Frequency, MHz	obs. –calc. kHz
K = 0–0			
7–8	1,7–1,8	112714.772	3
	1,8–1,9; 1,6–1,7	112715.330	–31
6–7	1,6–1,7	115388.242	13
	1,7–1,8; 1,5–1,6	115388.830	–29
5–6	1,5–1,6	118082.747	–9
	1,6–1,7; 1,4–1,5	118083.397	–1
4–5	1,4–1,5	120789.945	–32
	1,5–1,6; 1,3–1,4	120790.621	–20
3–4	1,3–1,4	123505.783	18
	1,4–1,5	123506.399	–7
	1,2–1,3	123506.661	90
2–3		–[b]	
1–2	1,2–1,2; 1,1–1,2	128974.656	–29
	1,2–1,3	128975.535	19
	1,1–1,1	128976.304	–9
0–1	1,1–1,1	131767.052	–41
	1,1–1,2	131768.215	–16
1–0	1,1–1,1; 1,2–1,1; 1,0–1,1	139049.329	25
K = 0–1(e)			
0–1	1,1–1,2	126812.865	–14
2–1	1,2–1,1; 1,3–1,2	139639.804	10
4–3	1,4–1,3	145470.189	56
	1,5–1,4; 1,3–1,2	145470.580	95
5–4	1,5–1,4	148459.980	–30
	1,6–1,5; 1,4–1,3	148460.445	27
8–7	1,5–1,4	158107.521	–12
	1,6–1,5; 1,4–1,3	158108.065	10
K = 0–1(f)			
1–1	1,1–1,0	132081.131	–22
	1,2–1,2	132082.106	65
	1,2–1,1; 1,1–1,1	132082.863	0
2–2	1,1–1,1	131637.338	56
	1,3–1,3	131637.982	31
	1,1–1,2; 1,3–1,2	131638.824	–29
	1,2–1,2	131639.150	–4
3–3	1,2–1,2	130973.212	–6
	1,4–1,4	130973.594	–74
	1,3–1,3	130974.949	–3
4–4	1,3–1,3	130091.534	–55
	1,5–1,5	130091.904	–24
	1,4–1,4	130093.248	2
	1,4–1,4	128997.080	–39
5–5	1,6–1,6	128997.371	–19
	1,5–1,5	128998.690	–30
6–6	1,5–1,5; 1,7–1,7	127697.170	25
	1,6–1,6	127698.610	41
7–7	1,6–1,6; 1,8–1,8	126201.690	20
	1,7–1,7	126203.075	7
8–8	1,7–1,7; 1,9–1,9	124524.704	–17
	1,8–1,8	124526.048	–40
9–9	1,8–1,8; 1,10–1,10	122684.352	5
	1,9–1,9	122685.700	21
10–10	1,9–1,9; 1,11–1,11	120703.756	–25
	1,10–1,10	120705.094	21
K = 2(f)–1(f)			
9–10	1,8–1,9; 1,10–1,11	117868.645	51
	1,9–1,10	117868.965	–53
8–9	1,7–1,8; 1,9–1,10	122230.646	–3
	1,8–1,9	122231.205	28
7–8	1,6–1,7; 1,8–1,9	126362.919	–64
	1,7–1,8	126363.587	–25
6–7	1,5–1,6; 1,7–1,8	130420.050	75
	1,6–1,7	130420.795	93
5–6	1,4–1,5; 1,6–1,7	134468.761	–102
	1,5–1,6	134469.644	–49
4–5	1,3–1,4; 1,5–1,6	138545.607	–68
	1,4–1,5	138546.547	–82
3–4	1,2–1,3	142676.037	–7
	1,4–1,5	142676.336	27
	1,3–1,4	142677.343	–8

Table 1 (*continued*)

$J'–J''$	$I', F'–I'', F''$	Frequency, MHz	obs. –calc. kHz
K = 2(f)–1(e)			
3–3	1,3–1,3	158054.271	32
	1,2–1,2; 1,4–1,4	158054.975	86
4–4	1,4–1,4	158008.020	101
	1,3–1,3; 1,5–1,5	158008.846	38
K = 2(e)–1(e)			
3–4	1,3–1,4	139728.143	–122
	1,2–1,3; 1,4–1,5	139728.877	–38
4–5	1,4–1,5;	135569.629	51
	1,3–1,4; 1,5–1,6	135570.487	80
5–6	1,5–1,6	131840.012	–44
	1,4–1,5; 1,6–1,7	131840.970	–2
6–7	1,6–1,7	128554.683	6
	1,5–1,6; 1,7–1,8	128555.634	0

[a] Experimental uncertainties estimated to be 50 kHz.
[b] This line was not measured because of overlap with a stronger transition.

The lowest $(j_{CO}, j_{N2}) = (0,1)$ state forms a pair of stacks with $K = 1$ corresponding to rotation of the N_2 subunit around the intermolecular axis and one stack with $K = 0$, which has the nature of a N_2 bending vibration. The energy levels of these stacks were well characterized by the microwave study [5]. The pure rotational $\Delta K = 0$ transitions (labeled by circles in the diagram) and $\Delta K = 1$ transitions were detected. It was shown that a strong Coriolis interaction occurs between $K = 0$ and $K = 1$ (e) levels [5].

The higher state of CO–*para*N_2 with excited rotation of the CO subunit, i.e. $(j_{CO}, j_{N2}) = (1,1)$, is more complicated. The free rotor picture predicts three $K = 0$ stacks, two pairs of $K = 1$ stacks, and one pair of $K = 2$ stacks. One pair, $K = 1$ (e) and $K = 1$ (f), was detected in our previous work [8] and the corresponding observed branches of transitions are shown in Fig. 1 by dotted lines. Solid lines represent newly observed subbands to three other upper stacks, $K = 0$ (e), $K = 2$ (e), $K = 2$ (f).

In total, 37 rotational transitions in the frequency range from 103 to 159 GHz were measured and assigned on the basis of molecular parameters from the infrared work of Rezaei et al. [9]. The transitions belong to P- and R-branches of the $K = 0–0$ subband, P-, R- and Q-branches of the $K = 0–1$ subband and P- and Q-branches of the $K = 2–1$ subband. Most of the observed lines display ^{14}N hyperfine structure. As an example, the $Q(2)$ $K = 0(e)–1(f)$ transition is shown in Fig. 2 together with a simulation of the spectrum obtained from the final set of spectroscopic parameters. The measured transitions frequencies, assignments, uncertainties and residuals are listed in Table 1. The quantum numbers are given using the coupling scheme $\mathbf{I} + \mathbf{J} = \mathbf{F}$, where $\mathbf{I}$ is the total nuclear spin angular momentum of the two equivalent nitrogen nuclei, $\mathbf{J}$ is the rotational angular momentum.

The newly determined line frequencies together with previously published microwave [5] and millimeter-wave [8] data on CO–*para*N_2 were used to fit simultaneously the band origins σ, the rotational and centrifugal distortion parameters and the nuclear quadrupole coupling parameters for $K = 0$, 1 in $(j_{CO}, j_{N2}) = (0,1)$ and $K = 0$, 1, 2 in $(j_{CO}, j_{N2}) = (1,1)$ states employing an exact diagonalization program [19]. The rotational and centrifugal distortion terms were expanded in $J(J+1) - K^2$ power series as in previous works [8,9]. The $K = 1(e)/(f)$ and $K = 2(e)/(f)$ doublets were fitted as two asymmetry components of one $K = 1$ or 2 state correspondingly using splitting term $\pm(\frac{1}{2})\{bJ(J+1) + d[J(J+1)]^2 + \ldots\}$ (plus sign for e and minus sign for f), where $b = 0$, for $K > 1$, $d = 0$ for $K > 2$, etc. In the case of $K = 1$, the parameters $b/2$, $d/2$, $h/2$, etc. used here correspond to $(B - C)/4$, d_1, h_1, etc. in the asymmetric rotor nomenclature. In the case of $K = 2$, the parameters $-d/2$, $-h/2$, etc. used here correspond to d_2, h_2 etc. in the asymmetric rotor nomenclature.

Table 2
Spectroscopic parameters (in MHz) of the observed states of CO–*para*N_2.

State		Previous[a]	Present
$(j_{CO}, j_{N2}) = (0,1)$			
$K = 0$	B	2122.74(354)	2143.34(59)
	D	0.417(53)	0.3121(44)
	$H \times 10^3$	0.96(21)	0.1611(48)
	$L \times 10^6$		0.282(58)
	χ_{aa}	−5.1115(18)[b]	−5.1726(99)
	$\chi_{aa,J} \times 10^3$		−4.40(95)
	$C \times 10^3$	9.9(95)/7.8(91)[c]	9.68(110)
$K = 1$	σ	4656.107(330)	4645.824(293)
	B	2187.86(170)	2177.446(293)
	D	0.0632(261)	0.11416(221)
	$H \times 10^3$	−0.488(102)	−0.10109(273)
	$L \times 10^6$		−0.2099(273)
	b	123.30(354)	144.024(586)
	d	−0.136(53)	−0.03898(442)
	χ_{aa}	0.5353(180)/ 0.5235(180)	0.5681(80)
	$\chi_{bb}(e)$	−0.0134(20)	0.0469(105)
	$\chi_{bb}(f)$	−3.0017(3)	−3.0353(85)
	$\chi_{bb,J}(f) \times 10^3$		4.34(77)
	$C(e) \times 10^3$	−18.7(25)/4.74(80)[d]	−7.43(109)
Interaction $K = 1(e)/G$ $K = 0$		2152.6(39)[g]	2176.10(66)
	G_J	−3.3709(267)	−3.3800(107)
	$G_{JJ} \times 10^3$		1.753(69)
$(j_{CO}, j_{N2}) = (1, 1)$			
$K = 1$	σ	102278.4553(188)	102278.4569(187)
	B	1996.7822(75)	1996.7885(74)
	D	−0.26810(82)	−0.27128(89)
	$H \times 10^3$	−1.590(35)	−1.591(35)
	$L \times 10^6$	7.38(62)	7.38(63)
	$M \times 10^9$	−0.0193(40)	−0.0190(41)
	b	−4.5304(62)	−4.53050(620)
	d	0.05556(64)	0.05558(66)
	$h \times 10^3$	−0.2378(206)	−0.2388(206)
	$l \times 10^6$	1.306(198)	1.326(100)
	χ_{aa}	−1.850(43)	−1.854(34)
$K = 0$	σ	134778.(3)	134772.7540(203)
	B	2137.005(306)	2138.4967(57)
	D	0.042(29)	0.11154(40)
	$H \times 10^3$	−0.6(33)	0.2825(106)
	$L \times 10^6$		−1.549(116)
	$M \times 10^9$		3.31(42)
	χ_{aa}		−0.734(45)
$K = 2$	σ	171730.(3)	171735.107(160)
	B	2297.663(351)	2297.461(33)
	D	0.3373(63)	0.33452(227)
	$H \times 10^3$		−0.333(69)
	$L \times 10^3$		0.01660(90)
	$M \times 10^6$		−0.1692(35)
	d	−0.1428(20)	−0.151216(570)
	$h \times 10^3$		0.3776(354)
	$l \times 10^6$		−7.926(526)
	χ_{aa}		1.037(122)
	$\chi_{2-} \times 10^3$		3.88(87)

[a] Rotational parameters for $(j_{CO}, j_{N2}) = (0,1)$ state from Xia et al. [6] and hyperfine structure parameters from Xu and Jäger [5]; for $(j_{CO}, j_{N2}) = (1,1)$ state from Rezaei et al. [9].
[b] A value of 8.440(68) was obtained for χ_{bb} in [5].
[c] Two values of C_{bb} and C_{cc} were obtained for $K = 0$ in [5].
[d] Two values of C_{bb} and C_{cc} were obtained for $K = 1(e)$; two values of 0.01149(74)/ −0.0330(24) were obtained for C_{bb} and C_{cc} for $K = 1(f)$ in [5].
[g] The values for G, G_J (and G_{JJ}) from [5,6] contain a factor of $\sqrt{2}$ as compared to values from Pickett's program.

Initially, we fit the $K = 1$ state of $(j_{CO}, j_{N2}) = (0,1)$ with separate sets of spectroscopic parameters for the (e) and (f) substates because of the very different hyperfine structure, as was done earlier [5,8]. In the present study, we follow Ref. [6,9] and treat both states as two asymmetry components of one $K = 1$ state. Even though we were able to employ a common χ_{aa} parameter, we needed to retain the very different remaining hyperfine parameters, as was the case in earlier studies [5,8]. The ^{14}N quadrupole coupling in $K = 1$ is expressed by two parameters. These are commonly χ_{aa} and χ_{bb} or χ_{aa} and χ_-, with $\chi_- = \chi_{bb} - \chi_{cc}$. The coupling in $K = 2$ is described analogously by χ_{aa} and χ_{2-}.

The interaction term $W = G[J(J+1)]^{1/2}$ was used to take into account a strong Coriolis interaction between $K = 1(e)$ component and $K = 0$ state as already known [5]. It was also found that inclusion of the centrifugal distortion corrections G_J, G_{JJ}, $\chi_{aa,J}$ or $\chi_{bb,J}$, as well as the spin-rotation constant C for $K = 0$ and 1 of the $(j_{CO}, j_{N2}) = (0, 1)$ state improved the quality of the fit substantially.

Each line consisting of overlapping hyperfine components was treated as the intensity weighted average of the individual components. Contributions of components weaker than the strongest one by more than a factor of 10 were not considered. Because of the overlap and the proximity of the hyperfine components, simulations were made to determine the differences between the intensity weighted average line positions and the apparent peak positions. Second derivatives line shapes were calculated in which each hyperfine component was represented by a Gaussian line profile of 300 kHz FWHM. The corrections applied were mostly below the 50 kHz uncertainties of the lines.

The spectroscopic parameters obtained for the new and previously observed states are given in Table 2. The parameters of the CO–*para*N_2 levels are in good agreement with previous values [5,6] for the lower $K = 0$ and $K = 1$ states. For the upper $K = 0$, $K = 1$ and $K = 2$ states the rotational constants agree reasonable with infrared study [9], but more centrifugal parameters were included in our fit. Quadrupole coupling parameters for these states were obtained for the first time in the present work. The weighted standard deviation of the fit was 0.674, suggesting slightly conservative judgment of the uncertainties. The scatter is small among the various subsets of the data.

3.2. CO–*ortho*N_2

For the CO–*ortho*N_2 spin modification we have observed five new P-branch transitions belonging to the $K = 0$–0 subband between $(j_{CO}, j_{N2}) = (1,0)$ and $(0,0)$ free rotor states. The lower $K = 0$ state represents the ground state of CO–*ortho*N_2 and the upper $K = 0$ has the nature of a CO bending vibration. The present observation involves $P(3)$, $P(4)$, $P(5)$, $P(6)$ and $P(7)$ lines in addition to $R(0)$, $R(1)$, $R(2)$, $R(3)$ and $P(1)$, $P(2)$ transitions measured in our previous work [7]. The transitions frequencies and assignments are listed in Table 3. Due to the limited number of new data for CO–*ortho*N_2 we do not perform here a new analysis for this spin modification, but these data may be used in a later global analysis.

4. Discussion and conclusions

In the case of the CO–*para*N_2 spin modification, the new information concerns the first observation of the rotational subbands

Table 3
Newly assigned $K = 0$–0 $(j_{CO}, j_{N2} = 1, 0–0, 0)$ rotational transitions of the CO–*ortho*N_2 complex and their frequencies.[a]

$J'–J''$	$I', F'–I'', F''$	Frequency, MHz
2–3	2,2–2,3; 2,3–2,4	125718.240
	2,4–2,5; 2,1–2,2; 2,0–3,1; 0,2–0,3	125718.780
3–4	2,2–2,3; 2,3–2,4	120467.348
	2,4–2,5; 2,5–2,6; 2,1–2,2; 0,3–0,4	120467.878
4–5	2,2–2,3; 2,3–2,4	114969.106
	2,4–2,5; 2,5–2,6; 2,6–2,7; 0,4–0,5	114969.672
5–6	2,3–2,4; 2,4–2,5;	109237.213
	2,5–2,6; 2,6–2,7; 2,7–2,8; 0,5–0,6	109237.815
6–7	2,4–2,5; 2,5–2,6;	103288.350
	2,6–2,7; 2,7–2,6; 2,8–2,7; 0,6–0,7	103288.942

[a] Experimental uncertainties estimated to be 50 kHz.

Table 4
Comparison of rotational constants B and nuclear quadrupole coupling parameters χ_{aa} of CO–N_2.

Spin modification	Stack (j_{CO}, j_{N2}, K)	B, MHz	χ_{aa}, MHz
CO–*ortho*N_2	(0,0,0)	2227.542[a]	0.21[a]
CO–*ortho*N_2	(1,0,1)	2141.982[a]	−1.04[a]
CO–*ortho*N_2	(1,0,0)	2089.750[b]	−0.77[b]
CO–*para*N_2	(0,1,0)	2143.34[c]	−5.17[c]
CO–*para*N_2	(0,1,1)	2177.446[c]	0.57[c]
CO–*para*N_2	(1,1,1)	1996.789[c]	−1.85[c]
CO–*para*N_2	(1,1,0)	2138.497[c]	−0.73[c]
CO–*para*N_2	(1,1,2)	2297.461[c]	1.04[c]

[a] Surin et al. [8].
[b] Surin et al. [7].
[c] Present work.

to the $K = 0$ and 2 stacks of the $(j_{CO}, j_{N2}) = (1,1)$ internal rotor state. This confirms recent infrared results [9] and leads to more accurate determinations of the relevant energy levels. Additional data provided by the current millimeter-wave spectroscopic survey concern hyperfine splitting of the observed levels.

In previous microwave and millimeter-wave studies [3–5,7,8] the information from hyperfine splitting and isotopic substitution was used for proposition of qualitative structures of CO–N_2 in different K-states. The microwave study of Xu et al. [4] revealed that the ground state $K = 0$ of CO–*ortho*N_2 has an approximate T-shaped structure with N_2 forming the top and CO forming the leg, and that the oxygen atom is closer to the N_2 unit than the carbon atom. The same study proposed that the lower $K = 1$ state of CO–*ortho*N_2 has a different geometry with N_2 forming the leg and CO forming the top. It was found that the negative value of χ_{aa} constant suggests that the N_2 subunit is more localized in the parallel direction with respect to the intermolecular axis, while the positive value of χ_{aa} indicates on the more perpendicular orientation of the N_2 subunit with respect to the intermolecular axis.

Table 4 summarizes the nuclear quadrupole constants χ_{aa} and rotational constants B for all known stacks in the ground vibrational state ($v_{CO} = 0$). Comparing these parameters, we can propose that the new $K = 0$ state of CO–*para*N_2 has a geometry similar to the lower $K = 1$ state of CO–*ortho*N_2, i.e. with N_2 forming the leg and CO forming the top. In contrast, the new $K = 2$ state has more similar B and χ_{aa} to the ground $K = 0$ states of CO–*ortho*N_2, thus assuming similar structure with N_2 forming the top and CO forming the leg.

As mentioned above, from free rotor picture we actually expect more stacks of levels arising from $(j_{CO}, j_{N2}) = (1,1)$ than detected: three $K = 0$, two pairs with $K = 1$, and one stack with $K = 2$. The negative values of the b and D constants of only one observed $K = 1$ stack indicates on possible interactions with some of the missing stacks. At the same time, a free rotation interpretation can be only partly valid. It seems neither specific fixed structures nor free internal rotation are really satisfactory descriptions for CO–N_2. In this respect, it would be very interesting to have dynamical calculations of rotational energy levels and wave functions for CO–N_2 using existing [15] or new interaction potentials. Numerous highly accurate experimental data are available already for direct comparison with possible future theoretical studies.

Acknowledgments

The work was supported by the Deutsche Forschungsgemeinschaft (DFG) through research grant SU 579/1. L.A.S. acknowledges support of the Russian Foundation for Basic Research (Grant 12-03-00985-a). A.P. acknowledges support from DFG via SFB 956.

References

[1] Y. Kawashima, K. Nishizawa, Chem. Phys. Lett. 249 (1996) 87.
[2] Y. Xu, A.R.W. McKellar, J. Chem. Phys. 104 (1996) 2488.
[3] Y. Kawashima, Y. Ohshima, Y. Endo, Chem. Phys. Lett. 315 (1999) 201.
[4] Y. Xu, W. Jäger, L.A. Surin, I. Pak, V.A. Panfilov, G. Winnewisser, J. Chem. Phys. 111 (1999) 10476.
[5] Y. Xu, W. Jäger, J. Chem. Phys. 113 (2000) 514.
[6] C. Xia, A.R.W. McKellar, Y. Xu, J. Chem. Phys. 113 (2000) 525.
[7] L.A. Surin, H.S.P. Müller, E.V. Alieva, B.S. Dumesh, G. Winnewisser, I. Pak, J. Mol. Struct. 612 (2002) 207.
[8] L.A. Surin, A.V. Potapov, H.S.P. Müller, V.A. Panfilov, B.S. Dumesh, T.F. Giesen, S. Schlemmer, J. Mol. Struct. 795 (2006) 198.
[9] M. Rezaei, K.H. Michaelian, N. Moazzen-Ahmadi, A.R.W. McKellar, J. Phys. Chem. A 117 (2013) 13752–13758.
[10] A.V. Potapov, L.A. Surin, V.A. Panfilov, B.S. Dumesh, T.F. Giesen, S. Schlemmer, P.L. Raston, W. Jäger, Astrophys. J. 703 (2009) 2108–2112.
[11] P. Jankowski, L. Surin, A. Potapov, S. Schlemmer, A.R.W. McKellar, K. Szalewicz, J. Chem. Phys. 138 (2013) 084307.
[12] K.A. Franken, C.E. Dykstra, J. Phys. Chem. 97 (1993) 11408.
[13] J. Fišer, R. Polák, Chem. Phys. Lett. 360 (2002) 565.
[14] J. Fišer, T. Boublík, R. Polák, Mol. Phys. 101 (2003) 3409.
[15] M.H. Karimi-Jafari, A. Maghari, A. Farjamnia, J. Phys. Chem. A 115 (2011) 1143.
[16] L.A. Surin, B.S. Dumesh, F. Lewen, D.A. Roth, V.P. Kostromin, F.S. Rusin, G. Winnewisser, I. Pak, Rev. Sci. Instrum. 72 (2001) 2535.
[17] L. Surin, A. Potapov, V. Panfilov, B. Dumesh, G. Winnewisser, J. Mol. Spectrosc. 230 (2005) 149–152.
[18] L.A. Surin, D.N. Furzikov, T.F. Giesen, S. Schlemmer, G. Winnewisser, V.A. Panfilov, B.S. Dumesh, G.W.M. Vissers, A. van der Avoird, J. Phys. Chem. A 111 (2007) 12238–12247.
[19] H.M. Pickett, J. Mol. Spectrosc. 148 (1991) 371.